Journal of The Electrochemical Society, **156** (4) B532-B539 (2009)
0013-4651/2009/156(4)/B532/8/$23.00 © The Electrochemical Society

Cross-Linker Effect in ETFE-Based Radiation-Grafted Proton-Conducting Membranes

II. Extended Fuel Cell Operation and Degradation Analysis

Hicham Ben youcef,[a] Lorenz Gubler,[a,z] Tetsuya Yamaki,[b] Shin-ichi Sawada,[b] Selmiye Alkan Gürsel,[a,c] Alexander Wokaun,[a] and Günther G. Scherer[a]

[a]*Electrochemistry Laboratory, Paul Scherrer Institut, Switzerland*
[b]*Japan Atomic Energy Agency, Quantum Beam Science Directorate, Takasaki, Gunma 370-1292, Japan*

In this study, the effect of cross-linker content on the chemical stability of poly(ethylene-*alt*-tetrafluoroethylene) (ETFE)-based radiation-grafted and sulfonated membranes was investigated. An ex situ degradation test in H_2O_2 solution showed a strong increase in stability of cross-linked membranes compared to uncross-linked ones. Excessive cross-linking, however, is detrimental to the chemical and mechanical properties. Furthermore, the stability of grafted membranes based on ETFE was superior to those based on poly(tetrafluoroethylene-*co*-hexafluoropropylene) (FEP). An in situ long-term test in a H_2/O_2 single cell over 2180 h, using an ETFE-based grafted membrane optimized with respect to cross-linker content, with a graft level of 25% was carried out. The performance of the membrane electrode assembly exhibited a voltage decay rate of 13 $\mu V\ h^{-1}$ over the testing time at a current density of 500 mA cm^{-2} and a cell temperature of 80°C, while the hydrogen permeation showed a steady increase over time. This indicates that, to some extent, changes in the membrane morphology occur over the operating period. Local postmortem analysis of the tested membrane reveals that high degradation was observed in areas adjacent to the O_2 inlet and in other areas nearby.
 [DOI: 10.1149/1.3082109]

Manuscript submitted November 25, 2008; revised manuscript received January 21, 2009. Published February 23, 2009.

The development of cost-effective proton exchange membranes to replace the state-of-the-art and expensive perfluorinated membranes (e.g., Nafion, Flemion, and Aciplex) is one of the main challenges on the road to commercialization of polymer electrolyte fuel cell technology. The radiation-induced grafting technique, based on the utilization of a low-cost base polymer material with either fluorinated or partially fluorinated polymer films, offers several advantages.[1] The radiation-induced grafting in combination with further chemical modification steps (sulfonation) allows the functionalization of the base material and the introduction of the desired property (proton conductivity). The attractiveness of this technique is based on its versatility and the possibility to easily control the grafting parameters (irradiation dose, concentration of monomers, time, temperature, solvent type, etc.). We can tune the desired membrane properties in a broad range due to the wide selection and combination possibilities of base films and grafting monomers.

One of the main research areas in our laboratory at the Paul Scherrer Institut is the development of low-cost polymer electrolyte membranes. Radiation-grafted membranes based on grafted styrene/divinylbenzene (DVB:cross-linker) onto poly (tetrafluoroethylene-*co*-hexafluoropropylene) (FEP) exhibited performance comparable to that of commercial Nafion 112 membranes and were able to operate over 4000 h without notable degradation under steady conditions at a temperature of 80°C.[2,3]

The FEP-based membrane was optimized with respect to its performance and chemical stability by adjusting the graft level and cross-linker content. In a study of the effect of DVB on fuel cell performance, the membrane prepared with 10% DVB (in the initial solution) was found to exhibit the best performance.[3] Recently, partially fluorinated poly(ethylene-*alt*-tetrafluoroethylene) (ETFE) has been identified as a promising alternative base polymer film because of its advantages (superior mechanical properties, better resistance to irradiation-induced damage, improved grafting kinetics) in comparison to the use of FEP as base film.[4] First fuel cell tests with styrene/DVB-grafted ETFE (25 μm)-based membranes, prepared using the same conditions as for the optimized FEP-based membranes, were reported earlier.[5]

The obtained results showed the potential of ETFE as base material, but still the system needed to be optimized regarding both key parameters, i.e., the graft level[d] (GL) and the cross-linker content. Subsequently, a detailed study on the influence of grafting parameters and reaction kinetics was performed for the grafting of styrene onto ETFE and, as expected, differences in kinetics in comparison to the combination of styrene and FEP were observed.[6] The influence of cross-linker was investigated, and a correlation between the DVB content and the ex situ relevant properties for fuel cells was established.[7]

The mechanical stability of our grafted films and membranes is a crucial prerequisite in terms of handling, fabrication, and durability of the membrane electrode assembly (MEA). Especially, the mechanical properties and dimensional stability (expansion/shrinkage of membrane area and volume due to changes in hydration state), which are influenced by the GL, cross-linker, and water content, are important features to characterize.[8] An evaluation of the effect of irradiation dose, GL, and cross-linking was performed, and a comparison with a Nafion 112 membrane was established.[9] It was found that a careful balance of all these parameters is needed to reduce their negative impact on the elongation at break and tensile strength.

Our group focused not only on styrene-based grafted membranes but also on different monomer combinations in order to improve the chemical stability under fuel cell operating conditions. For that aim, alternative styrene-derived monomers with protected α-position were chosen, such as α,β,β-trifluorostyrene derivatives[10] and α-methylstyrene/methacrylonitrile.[11] In our approach, the in situ test of our materials is the key tool for evaluating membrane for performance and durability.

The influence of the GL and degree of cross-linking on the ex situ and in situ properties of the grafted ETFE-based membranes was investigated in detail in our previous article.[5,12] Based on these earlier findings, an increasing GL was observed to lead to more brittle membranes, whereas a low GL does not afford good conductivities. The optimum GL was identified to lie between 24 and 30%. In this compositional range, the mechanical integrity, conductivity, and performance of the grafted membranes are well-balanced.[5] Moreover, it was found that the water uptake and the conductivity were negatively affected by an increase of the cross-linker content as a consequence of the formation of an increasingly tight polymer

[c] Present address: Faculty of Engineering and Natural Sciences, Sabancı University, 34956 Istanbul, Turkey.
[z] E-mail: lorenz.gubler@psi.ch

[d] GL (or degree of grafting) = $(m_g - m_0)/m_0$, where m_0 and m_g are the sample masses before and after grafting, respectively.

network. In addition, cross-linking results in an increase of the brittleness and likelihood of membrane cracking during MEA preparation or operation. Fuel cell tests of a membrane prepared using a cross-linker content of 5% DVB in the initial grafting solution were found to yield maximum performance.[12] At lower extents of cross-linking, performance is limited by the poor membrane–electrode interfacial properties, whereas at higher degrees of cross-linking, performance is limited by high ohmic resistance of the membrane.

In the present study, a cross-linked ETFE-based membrane, which has previously been optimized for performance,[12] with a GL of 25% was evaluated for durability. In addition, the effective cross-linker (DVB) content of the grafted film was determined by Fourier transform IR (FTIR) spectroscopy, which was already pointed out to be different from the concentration in the initial grafting solution previously.[7] The obtained membrane was then characterized for its fuel cell relevant properties (ion exchange capacity, water uptake, conductivity, etc.), and a long-term fuel cell test was carried out. The MEA was intermittently characterized over the testing period, and the in situ properties were determined using auxiliary current-pulse resistance, electrochemical impedance spectroscopy (EIS), polarization, and H_2 permeation measurements. Furthermore, a local postmortem analysis using FTIR was performed to yield a degradation map over the active area.

Experimental

Membrane preparation and composition determination.— Radiation-grafted membranes based on Tefzel ETFE 100LZ film (DuPont, Circleville, OH, USA) with 25 μm thickness were prepared using the procedure reported earlier.[7] ETFE films were electron-beam irradiated at a dose of 1.5 kGy and subsequently stored at −80°C until used. A monomer solution composed of styrene (purum grade; Fluka) and DVB (technical grade, ~80%, mixture with isomers 3- and 4-ethylvinylbenzene; Fluka) with varying styrene:DVB ratio (v/v) was prepared. This monomer mixture was added to the solvent mixture prepared from isopropanol (analytical grade; Fisher Scientific) and water at a ratio of 11:5 (v/v). Grafting was carried out in a stainless steel reactor at a temperature of 60°C. The GL was adjusted to ~25% by varying the grafting time accordingly.

The cross-linker (DVB) content was determined by FTIR using a Perkin Elmer FTIR System 2000 spectrometer. GRAMS/386 software (version 3.02) from Galactic Industries was used for the curve fitting of the obtained FTIR spectra. The molar ratio of DVB/styrene determination was based on the fact that the styrene and the DVB isomers (para- and meta-disubstituted benzene) have distinct and unique bands at 1486 cm^{-1} (meta-disubstituted benzene), 1493 cm^{-1} (mono-substituted benzene), and 1510 cm^{-1} (para-disubstituted benzene). The molar ratio was then calculated based on developed calibration curves for the different bands (unpublished method).

Mechanical properties.— The mechanical properties of the membranes were measured by a Universal Testing Machine (Zwick Roell Z005) with a maximum test load of 5 kN. The measurements were performed at a cross head speed of 100 mm min^{-1}. The membranes were converted to salt form in KCl solution (0.5 M) and then dried at 60°C in an oven for 24 h. Rectangular specimens (1 × 10 cm) were die cut.

Ion exchange capacity, water uptake, and conductivity.— The sulfonation to yield proton-conducting membranes was carried out by treating the grafted films with chlorosulfonic acid in dichloromethane [2% (v/v)] at room temperature for 5 h, followed by hydrolysis in 0.1 M NaOH solution and reprotonation in 2 M H_2SO_4 solution. Finally, the resultant membranes were swollen in deionized water at 80°C for 5 h. The ion exchange capacity (IEC) was determined after cation exchange in KCl solution (0.5 M) by acid-base titration using KOH solution (0.05 M). The water uptake was determined from the difference in weight between the fully swollen and the dry membrane. The proton conductivity was measured for fully swollen membranes at room temperature via ac impedance spectroscopy using a Zahner IM6 (Kronach, Germany) in the frequency range of 1–50 kHz. For details on the experimental procedures used for ex situ characterization of the grafted membranes, the reader is referred to Ref. 5.

Single fuel cell testing and in situ characterization.— The ETFE- based membrane with a GL of 25.2% and cross-linked using 5% DVB (v/v) monomer in the grafting solution was hotpressed together with ELAT electrodes (type LT140EWSI, BASF Fuel Cell, Inc.) with a platinum loading of 0.5 mg cm^{-2} at 110°C/5 MPa/180 s to form an MEA. The MEA was assembled into a single cell (active area: 29.2 cm^2) comprising a threefold serpentine flow field (graphite plates) with channel/land width of 1 mm and channel depth of 0.5 mm.[12] The electrochemical characterization methods (polarization curves, impedance spectroscopy, H_2 permeation) used for MEA evaluation and the procedures are explained in detail in the first part of our contribution.[12]

Ex situ chemical degradation.— Membrane samples were dried in the oven under vacuum, then weighed and immersed in ultrapure water overnight (water-equilibration step). Subsequently, the samples were inserted into glass beakers containing a 3% H_2O_2 aqueous solution and treated for different periods of time at 60°C. The samples were then removed, immersed again in pure water and agitated for more than 24 h. The final step was to dry the rinsed membranes in the oven under vacuum overnight, after which they were weighed for the second time.[13] The residual weight R of the membrane after exposure to the H_2O_2 solution for a given period of time is calculated via the following equation

$$R(\%) = \frac{W_d(t)}{W_d(0)} 100\%$$

where $W_d(0)$ is the weight of the dry membrane at $t = 0$ and $W_d(t)$ is the weight of the dry membrane after H_2O_2 treatment.

Postmortem analysis.— After terminating the fuel cell test, the cell was disassembled and MEA ultrasound treated for 30 min to detach the electrodes from the membrane. The membrane was exchanged into salt form (K^+) by immersing in 0.5 M KCl solution overnight and then dried at 60°C for at least 16 h. A postmortem analysis by FTIR was performed in the nonactive and active area of the tested membrane by the use of a metallic slit mask (rectangular aperture 0.5 mm × 1.9 cm). With this slit width (0.5 mm), it is possible to determine the local degradation in the aged membrane, resolved to channel and land dimension (1 mm width) over the active area of the membrane.[14] A degradation map was created by measuring the extent of degradation over the 27 channels and 26 lands, with 7 measurements in each position along the channel/land. The area of the aromatic peak appearing at 1494 cm^{-1} assigned to styrene was measured to determine the extent of degradation according to

$$\text{Degradation}(\%) = \frac{\text{peak area(untested)} - \text{peak area(tested)}}{\text{peak area(untested)}} 100\%$$

Results and Discussion

Ex situ relevant properties of the ETFE-based membrane.— Based on our previous study on the effect of irradiation dose, GL, and cross-linking on different ex situ properties (thermal stability, mechanical stability, conductivity, etc.), a membrane optimized for performance based on radiation grafted styrene/DVB onto ETFE was defined. Furthermore, an investigation of the effect of cross-linker content on the in situ membrane properties (performance, resistance, interface, etc.) was carried out.[12] It was found that the maximum performance was reached using the membrane based on 5% DVB (v/v). The thickness of the obtained membrane was measured and the effective extent of cross-linking (DVB) determined by FTIR. The obtained value of the DVB/styrene molar ratio in the membrane is significantly (~50%) higher than the value in the ini-

Table I. Comparison of the DVB/styrene molar ratio in the initial grafting solution and in the grafted film measured by FTIR.

Membrane	GL (% wt)	Molar ratio (DVB/styrene) in the grafting solution (%)	Molar ratio (DVB/styrene) in the grafted film (%)	Thickness[a] (μm)
ETFE-25	25.2	4.3 ± 0.0	6.7 ± 0.1	34.0 ± 0.6
Nafion 112	—	—	—	58.0 ± 3.0

[a] Thickness measured for the membrane in liquid-water equilibrated state.

tial grafting solution (Table I). DVB is well known to be more reactive than styrene and, therefore, the consumption of DVB during the grafting reaction is faster than that of styrene.[15-17] Likewise, FTIR measurements show that the DVB is incorporated to a high degree close to the surface in comparison to the bulk of the grafted film [attenuated total reflection (ATR) vs transmission measurements].[7] The thickness of the resulting grafted ETFE-based membrane measured in the wet form is lower than that of the Nafion 112 membrane.

The mechanical properties of the resulting membrane converted to salt form were evaluated in dry state regarding both directions, machining (MD) and transverse direction (TD) (MD refers to the extrusion direction of the produced roll) (Table II). Previously, we have pointed out that grafting and cross-linking level play a pivotal role in the resulting mechanical properties of the radiation-grafted ETFE-based membrane. The study reveals that the parameter mostly affected is the elongation at break. Indeed, the brittleness of the ETFE-based grafted films and membranes increases drastically with the increase of the degree of grafting and cross-linking.[9] For both types of membrane, Nafion 112 and ETFE-based grafted membranes, the elongation at break and Young's modulus are higher in the TD than the values obtained in the MD, whereas the opposite is observed for the tensile strength (as expected from the orientation during the processing of the base film). The ETFE-based membranes show higher elongation at break and Young's modulus in both directions compared to the Nafion 112 membrane. The tensile strength of the ETFE-based membrane is higher in the transverse direction, while comparable values were measured in the machining direction. The correlation between mechanical properties determined ex situ and mechanical robustness of a membrane in a fuel cell environment is complex and not straightforward. In particular, time-dependent properties, such as viscoplastic creep and buildup of residual stress due to changes in membrane hydration, have to be taken into account and quantified, which does not seem to be a prominent topic in the scientific fuel cell literature. It is, however, evident that membranes with low elongation at break are unfavorable, as they tend to undergo brittle fracture. Currently, we are investigating in detail the tensile properties under fuel cell relevant conditions, i.e., at higher temperature and under controlled relative humidity conditions.

Table II. Mechanical properties of the ETFE-based membranes [GL ≈ 25.2%; molar ratio (DVB/styrene) ≈6.7%] and Nafion 112 membrane in both MD and TD.

Membrane	Direction	Elongation at break (%)	Tensile strength (MPa)	Young's modulus (MPa)
ETFE-25	MD	114 ± 15	50 ± 2	820 ± 47
	TD	139 ± 27	46 ± 2	844 ± 34
Nafion 112	MD	87.4 ± 8	50 ± 5	567 ± 22
	TD	126 ± 14	38 ± 2	575 ± 25

The ex situ properties (IEC, water uptake, conductivity, and hydration number) are fundamental characteristics for fuel cell performance. Representative results for the grafted ETFE-based membrane are compared to the values of Nafion 112 (Table III).[5] The Nafion 112 membrane shows higher water content and conductivity than the ETFE-based membrane, while the IEC value is lower (mass-based values). Furthermore, the IEC values, taking into account the difference in density between both types of membranes, were evaluated, and values of 2.4 and 1.6 mmol cm^{-3} for the ETFE-grafted membrane and for Nafion 112 membrane, respectively, were determined.[12] Nafion 112 is not a cross-linked membrane, and comparable water content and conductivity values were obtained for an uncross-linked styrene-grafted ETFE-based membrane at a GL of 25.6%. Thus, the lower water content in the ETFE-based membrane is a consequence of cross-linking, which was quantified previously by FTIR.

Ex situ chemical degradation.— The permeation of H_2 and O_2 through the membrane and interaction with the platinum electrocatalyst under fuel cell operating conditions results in the creation of peroxyl or hydroperoxyl radicals ($OH^{\bullet}$, $HOO^{\bullet}$), which are an aggressive degrading agent for the membranes.[18,19] One method to pre-evaluate the chemical stability of our membranes was to apply a moderate accelerated test, where an H_2O_2 solution is used instead of the severe Fenton reagent ($H_2O_2 + Fe^{2+}$), which leads to extensive $OH^{\bullet}$ generation and excessively fast membrane degradation.[13]

The influence of the DVB concentration on the chemical stability of the ETFE- and FEP-based membranes with fixed graft levels of ~25 and ~18%, respectively, were studied. Various membranes based on ETFE with different DVB contents (0, 5, 10, and 15% DVB in the initial grafting solution) and FEP membranes (0 and 10% DVB) were prepared and tested for their ex situ chemical stability by immersing them in a 3% H_2O_2 solution at 60°C. The IEC of all membranes was determined prior to the test, and the same value of around 1.6 mmol g^{-1} was measured for the ETFE membranes and a value of 1.3 mmol g^{-1} for the FEP-based membranes. The accelerated chemical degradation of these membranes was measured, and the evolution of the weight loss is depicted in Fig. 1. All the treated membranes show an onset of weight loss after some initial period, depending on the cross-linker concentration. Based on the measured GL and assuming a degree of sulfonation of 100%, the calculated weight loss due to total loss of the grafted components is in accordance with the experimental values at the end of the stability test. The weight loss is most likely a consequence of polymer chain scission occurring in the membranes, the fragments of which are washed out subsequently.[13] It was previously stated that the existence of radicals ($OH^{\cdot}$, $HOO^{\cdot}$) in the solution may result in an attack on the styrene unit, leading to the formation of a benzyl radical and,

Table III. Measured value of IEC, water uptake, hydration number, and conductivity of the ETFE-based membrane [GL ≈ 25.2%; molar ratio (DVB/styrene) ≈6.7%] compared with the values for Nafion 112 membrane.

Membrane	IEC (mmol g^{-1})	Conductivity[a] (mS cm^{-1})	Water uptake[a] (% wt)	Hydration number $[n(H_2O)/n(SO_3^-)]$
ETFE-25	1.6 ± 0.1	64 ± 3	20.6 ± 0.6	7.0 ± 0.5
Nafion 112	0.9 ± 0.1	82 ± 6	33.5 ± 1.8	18.0 ± 0.9

[a] Measurements were performed in fully swollen state at room temperature.

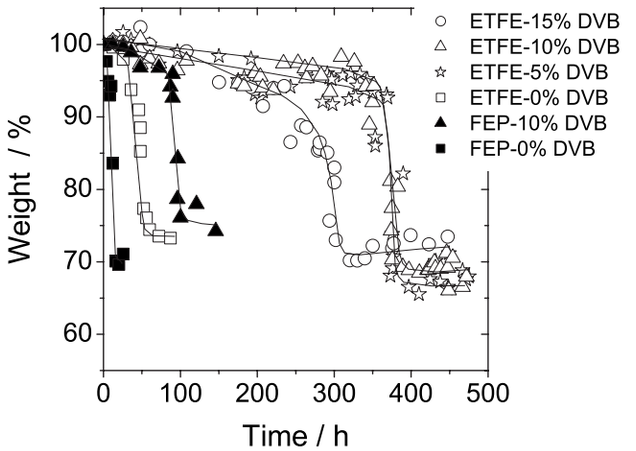

Figure 1. Ex situ chemical degradation of FEP-based membranes (GL ≈ 18%) and ETFE-based membranes (GL ≈ 25%) with different DVB contents (in the initial grafting solution) in 3% H_2O_2 at 60°C (lines are a guide for the eyes).

eventually, scission of the C–C bond of the grafted polymer chain.[19] Study of the decomposition products in the produced water from the fuel cell based on styrene grafted FEP membranes was performed earlier using high-pressure liquid chromatography, revealing mainly the formation of sulfonated aromatic residues.[20,21] Likewise, a Raman investigation of styrene-based grafted poly(vinylidene fluoride) membranes shows a loss of the poly(styrenesulfonic acid) groups after fuel cell tests.[18] Comparing the obtained results, the first main observation is that cross-linking generally induces an increase in the chemical stability of the ETFE- and FEP-based membranes. Also, the base polymer seems to have an effect on the durability of the grafted membrane; the cross-linked FEP-based membrane (10% DVB) appears to have the lowest stability among the cross-linked samples. A possible explanation can be related to the kinetics of grafting in both systems, in that the incorporation and content of cross-linker are different. Indeed, the values reported for water uptake and hydration number for the FEP membrane (10% DVB) are 16.3 wt % and ~6.7 water molecules per sulfonic group, respectively, whereas the values for ETFE (10% DVB) are lower (14.1 wt % and 4.6 water molecules per sulfonic group), suggesting that the effective cross-linking is higher in ETFE-based grafted membranes.[12] The observation that the ETFE-based membrane with the highest cross-linker content (15%) shows a lower stability compared to the membranes with lower DVB content is striking at first sight. Similar results were obtained, however, for ETFE (50 μm)-based membranes grafted with *p*-methylstyrene/ DVB. The increase of the DVB content above a critical concentration results in a drastic decrease in chemical stability.[22] Several factors may play a significant role in that observed behavior. In fact, higher cross-linker concentration in the grafting solution induces an increase in the number of pending double bonds in the grafted membranes as observed by FTIR, which affect the efficiency of the DVB as cross-linker.[23] Kinetic studies of the styrene/DVB system reveal that the reactivity of the two double bonds of DVB is not the same.[16] After the first double bond has reacted, the kinetic of the second one in the growing polymeric chain is much lower, yielding a fraction of unreacted double bonds in the final membrane. It has been proposed that the unreacted vinyl groups may be preferrable sites of radical attack.[22] The grafting kinetic dependency of styrene/DVB on the monomer diffusion and the relatively faster reaction of the DVB presumably create a concentration gradient through the membrane thickness. Indeed, the previously obtained FTIR-ATR results clearly show a higher DVB concentration close to the surface, whereas a comparatively lower cross-linker content is observed in the bulk of the membrane.[7] The higher extent of cross-linking may also produce a

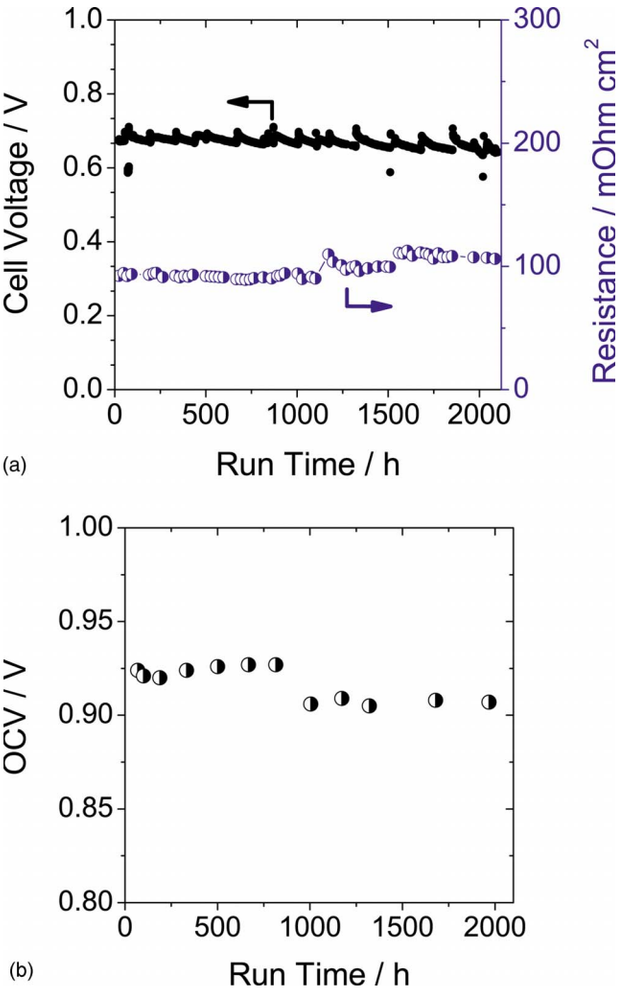

Figure 2. (Color online) (a) Single-cell durability test using a radiation-grafted membrane based on ETFE (GL 25%, 5% DVB). (b) Evolution of the OCV over the testing time. Measurements at 500 mA cm^{-2}, cell temperature 80°C; H_2/O_2 at a stoichiometry of 1.5/1.5, atmospheric gas pressure.

higher number of chain ends; consequently, the probability to form polymer branches with lower molecular weight (lower chain-length), which are more easily detached from the polymer network, in the membrane might be higher.

Fuel cell durability test.— After assembling the grafted ETFE-based membrane (5% DVB) into the fuel cell, an MEA durability test was performed at a constant current density of 500 mA cm^{-2}. The cell performance, as indicated by the cell voltage, and the ohmic membrane resistance measured by the pulse method are shown in Fig. 2a over the testing time. The evaluated drop in voltage after 1100 h was around 11 mV, whereas this value was about 21 mV at the end of the test (2180 h). Linear regression analysis of the voltage over the testing time yields a voltage decay rate of 13 μV h^{-1}. Looking more closely at the history plot, the MEA history can be divided into two intervals with different voltage decay rates, the first occurring from the beginning of the test up to 1100 h with a value of 7 μV h^{-1} and a second from 1100 to 2100 h with a decay rate of 23 μV h^{-1}. Concerning the ohmic resistance, no change was noticed for the pulse-measured ohmic resistance up to 1100 h, whereas an increase of 6% was observed up to 1508 h, and then a further increase of 7% was measured up to 2100 h. The membrane resistance increased from initially 94.5 to ~ 100 mΩ cm^2 after 1100 h and then reached a value of

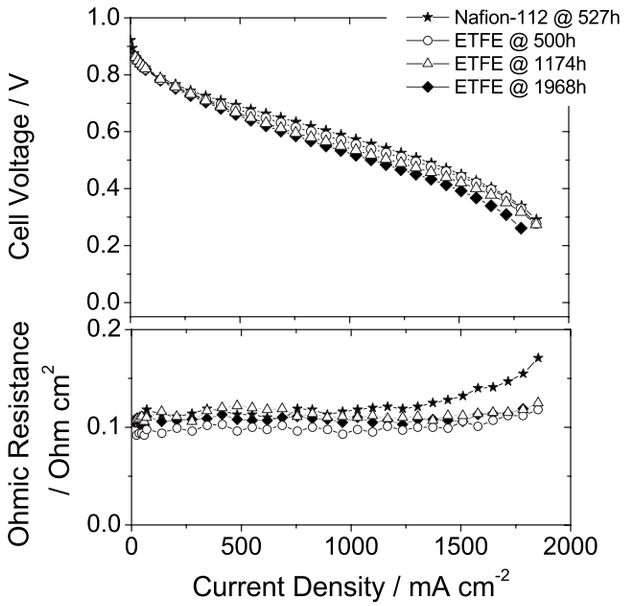

Figure 3. Polarization curves recorded at different times of the durability test for the cell with ETFE-based membrane (Fig. 2), compared to a cell with Nafion 112 membrane.

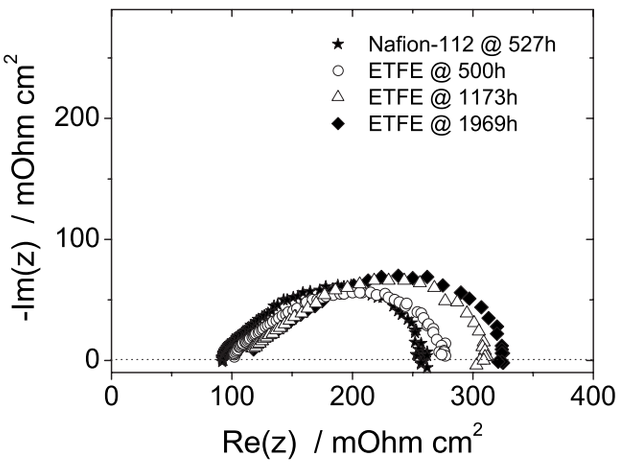

Figure 4. AC impedance spectra recorded at a dc current density of 500 mA cm^{-2} after different run times shown in the Nyquist representation (frequency range: 0.1 Hz to 25 kHz).

$\sim$106 mΩ cm^2 at the end of the test. Both stepwise changes in resistance were observed after restarting the cell (after measuring the H_2 crossover in H_2/N_2 mode and refilling of the bubbler humidifiers), which may indicate the adverse effect of start–stop cycles and their association with degradation phenomena in our system.[2]

The polarization curves obtained over the testing time are shown (Fig. 3). The performance of the ETFE-based membrane and the Nafion 112 after about 500 h of operating time shows similar results. However, the measured pulse ohmic resistance of the Nafion 112 was slightly higher, even showing a marked increase at high current densities starting from 1250 mA cm^{-2}. This may be the result of a stronger dehydration by the effect of electro-osmotic drag on the anode side, which induces an increase in the area resistance.[21] Moreover, the difference in membrane microstructure, the water transport mechanism, and the membrane–electrode interface may be influential parameters.[5,21] The ohmic resistance does not show any significant change up to 1174 h, where after an increase leading the ETFE-based membrane to reach the same values as those of the Nafion 112 was observed after 1968 h. However, the ETFE-based membrane does not show any marked increase in resistance at high current densities, as observed for the Nafion 112, over the testing time.

The extracted open-circuit voltage (OCV) values at various operating times for the MEA are shown (Fig. 2b). The first general observation is that the OCV values show two distinct levels. The first one starts from the beginning up to 815 h, whereas the second one starts from 1004 h until the end of the test. Moreover, the OCV slightly decreased from 0.924 V measured at 68 h to a value of 0.920 V at 188 h, which is assumed to be a consequence of the time needed for the cell and the interface of the MEA to run in. The observed trend for the OCV correlates with the measured changes in the decay rates of the cell voltage, indicating that the event at around 1000 h adversely affected membrane integrity.

In order to resolve the different losses occurring within the MEA, EIS was performed intermittently over the testing period (Fig. 4). From the electrochemical impedance spectra, the ohmic resistance was determined from the intersection of the impedance spectrum with the real axis at the high-frequency end, whereas the polarization resistance was obtained by subtracting the ohmic resistance from the resistance value at the intersection of the spectrum with the real axis at the low-frequency end.

The Nafion 112-based MEA exhibits both lower ohmic and polarization resistance in comparison to the MEA with grafted ETFE membrane. The higher interfacial resistance (polarization resistance) in the case of the ETFE-based membrane was already pointed out to be mainly due to the lower compatibility of these grafted membranes to the Nafion ionomer used in the catalyst layer of the electrodes.[12] The resistance values extracted from the ac impedance spectra are depicted in Fig. 5. The ohmic resistance does not show any change up to 800 h, whereas a slight increase of $\sim$4% after 1200 h was observed. The polarization resistance of the ETFE-based membrane decreases slightly up to 500 h and then increases after 800 and 1200 h, after which no significant change is observed. The observed slight decrease in the polarization resistance up to 500 h is most probably due to the improvement of the membrane–electrode interface during run-in. The extracted data of both resistances shows an increase after 1200 h, which is a sign of deterioration of the

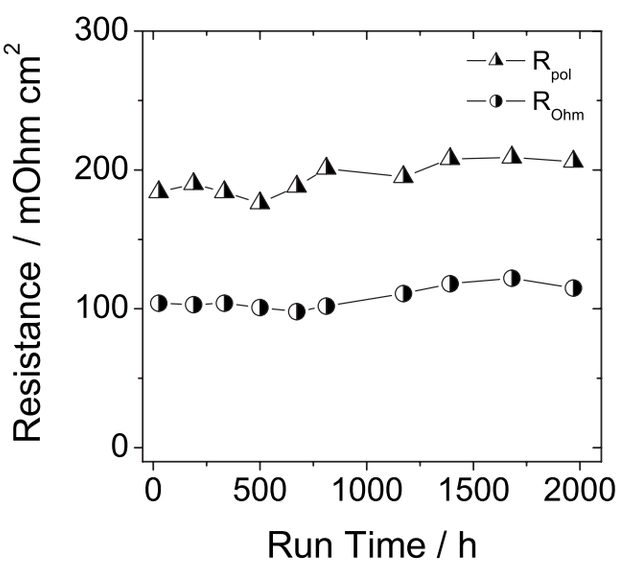

Figure 5. Extracted ohmic (R_Ω) and polarization resistance (R_{pol}) from the EIS spectra at 500 mA cm^{-2}.

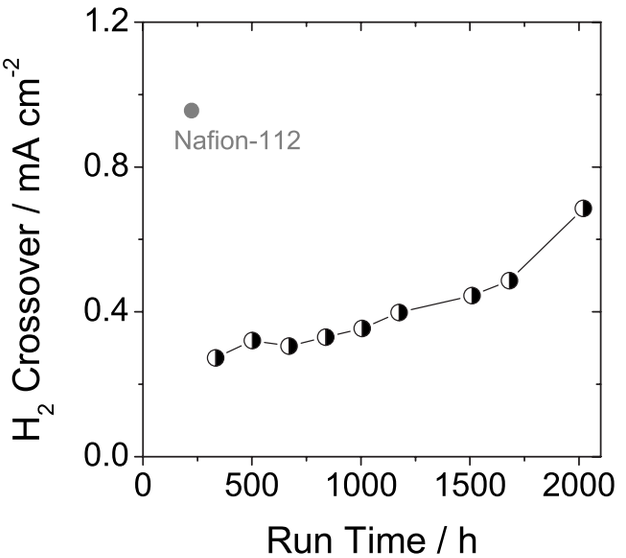

Figure 6. Hydrogen crossover measured electrochemically in H_2/N_2 mode at 80°C.

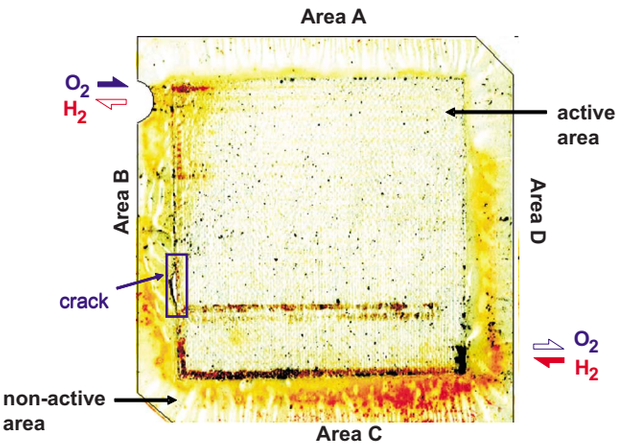

Figure 7. (Color online) Scanned image (contrast enhanced) of the membrane disassembled from the MEA after 2180 h on test.

MEA. Moreover, the obtained results are in accordance with the observed loss in the OCV at 1000 h, due to the sensitivity of the membrane to start–stop events. The absolute ohmic resistance values determined by EIS are slightly higher than the values measured by the current-pulse method due to the effect of cable inductance during measurements at high frequency.

It was also important to investigate the H_2 crossover of the ETFE-based grafted membrane over the testing time due to the close cause–effect relationship existing between the rate of chemical degradation and possible changes in the morphology of the membrane and its mechanical integrity (Fig. 6). The hydrogen crossover shows a steady increase with testing time up to 2000 h, and a corresponding H_2 permeation rate of >30 mA cm^{-2} was observed at the end of the test after 2180 h. These results indicate clearly that, to some extent, changes in the membrane morphology and integrity occur over the operating time, in accordance with other measured in situ parameters (performance, ohmic, and polarization resistances) (see Fig. 2 and 5). Dealing with a grafted membrane, the water management and the hydration–dehydration states become crucial issues in durability and mechanical integrity. Likewise, water is known to play the role of a plasticizer, allowing more mobility of the chains. Therefore, the combination of morphological changes and the chemical degradation of the graft components (see postmortem results) may be responsible for the observed increase in gas permeation. The correlation of this result with the extent of degradation occurring in the membrane is discussed in the next section.

Postmortem analysis.— The durability test was discontinued after a total testing time of 2180 h. The cell was subsequently disassembled, and the membrane was separated from the electrode by immersing the MEA in water and using ultrasound to promote delamination (Fig. 7). The first observation is that the membrane showed a crack of about 1.5 cm length in the edge zone (the border between the active and nonactive area). In fact, pinhole formation was suspected from the sudden drop in performance near the end of the test and the measured H_2 crossover (>30 mA cm^{-2}). Therefore, the correlation between the chemical degradation (postmortem analysis), performance drop, and the observed mechanical failure was of high interest.

To evaluate the local extent of degradation in the nonactive area (not assembled with the electrodes) (areas A, B, C, and D as shown in Fig. 7), selected points of the membrane were measured by FTIR (Table IV). Area B shows marked degradation in comparison with the other nonactive zones, while both areas A and D show similar trends, and lower degradation was observed. Interesting results were determined for the area near the hydrogen inlet of the tested membrane (area C), where degradation was low. These results are somewhat surprising; previously this area (nonactive) was used as a reference for the evaluation of the degradation, because no deterioration was claimed to occur there.[24] Furthermore, the marked difference in the extent of degradation between area B and the rest of the nonactive area is not yet understood. The strong degradation in zone B can be correlated with the membrane crack formation in that area. Furthermore, the notable chemical degradation in peripheral areas is also assumed to be due to propagation of peroxides in these areas or existence of other phenomena which occur in the presence of potential contaminants (e.g., Fe) and H_2/O_2.

The degradation within the active area was quantified on the channel and land scale (53 positions in total). Seven points in the lateral direction were measured for each channel and land, and the obtained degradation profile is presented in Fig. 8. There appear to be distinct areas of high degradation (50–60%), whereas a large fraction, particularly on the lower half of the active area near the H_2 inlet, show moderate degradation of 12% on average. Strong degradation was observed in the first serpentine (positions 53 and 52) located near the O_2 inlet, between positions 41 and 43 and at position 31 (channel). The obtained results do not show any significant difference or clear trend between the degradation in channel and land positions in the area of moderate degradation. If we consider the overall area, we find that the extent of degradation in the channel areas (18%) was somewhat higher than in the land areas (13%), due to the channel positions with high degradation near the O_2 inlet. A similar observation was already made for aged FEP-based grafted membranes, where a high degradation in channels was observed after an OCV hold test.[14] The local degradation of membranes on the sub-millimeter scale may strongly depend on the operating conditions.[25] The phenomenon has not been investigated in great detail up to now, yet it has been established that substantial differences in local conditions (O_2 content, temperature, potential, current density, and hydration state of the membrane) may exist across channel and land.[26,27]

Table IV. Measured degradation in the nonactive area for areas A, B, C, and D.

	Area A	Area B	Area C	Area D
% Degradation	38 ± 14	82 ± 14	10 ± 6	38 ± 10

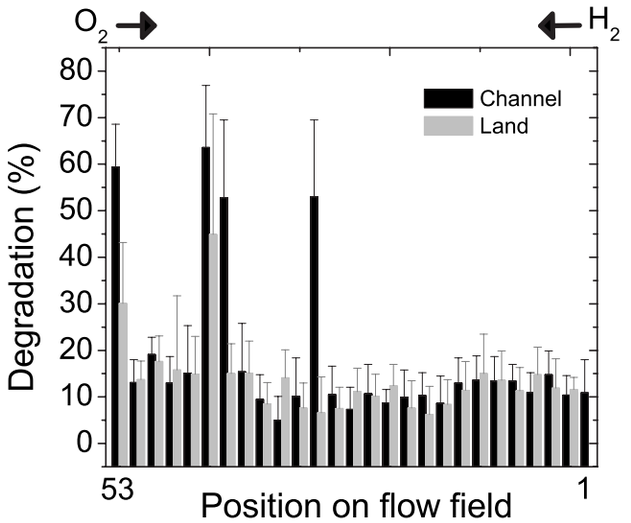

Figure 8. Local degradation analysis of the ETFE-based membrane in areas associated with flow-field channels and lands, determined via locally resolved postmortem FTIR spectroscopic analysis.

An overall representation of the local differences in the extent of degradation is shown in the degradation map of Fig. 9. In addition to the findings discussed in the previous paragraph, there appears to be a lack of correlation between the highly degraded zones and the crack location in the membrane, which is at the edge of the active area in the lower half. Consequently, the crack forming in our case may be assumed to be due to mechanical failure of the membrane near the end of the test because of mechanical stress in this area between the hydrated active and nonhydrated inactive area. Likewise, electrode misalignment may also explain the observed crack in the edge zone. Indeed, membrane failure was found to occur systematically in the perimeter region of the active area, where there may be an overlap of one electrode over the other.[28]

The presented durability test based on the ETFE-grafted membrane (5% DVB) was reproduced with the use of a 25 μm Kapton film as a subgasket as an additional protection against the observed edge effect. The cell was operated for more than a thousand hours without any noticeable increase in membrane resistance.

Conclusion

The ex situ chemical-degradation investigation revealed that the base film has an influence on the stability of radiation-grafted membranes. Higher stability was observed for the ETFE-based membrane over the FEP-based one. In addition, low and medium extents of cross-linking yield an improvement in the stability of the grafted membranes, yet at high cross-linker content a decrease is observed. A fuel cell membrane based on an optimized styrene/DVB grafted ETFE membrane with a graft level of 25% was characterized for its ex situ relevant fuel cell properties (IEC, water uptake, conductivity, and mechanical properties). The conductivity and water uptake of the grafted membrane were shown to be lower than that of Nafion 112, while the IEC shows an opposite trend, which is mainly attributed to the different densities and the effect of cross-linking and reduced free volume available within the polymer structure of the grafted membrane. Furthermore, the ETFE-based membrane shows slightly superior mechanical properties in terms of elongation at break and tensile strength.

A durability test with the optimized ETFE-based membrane was performed in a single fuel cell over a testing period of 2180 h. The MEA shows two regimes in cell voltage loss up to 2100 h, where a sudden drop was observed after 2180 h due to crack formation in the membrane. Moreover, the tested cell shows comparable performance to that of a Nafion 112-based cell, and only a slight decrease in performance at high current densities was observed up to 2000 h. Postmortem analysis reveals that degradation is strongly localized, with more degradation near the O_2 inlet, and the membrane areas associated with flow-field channels were more affected than the respective land areas. It was found that degradation occurred in the nonactive area to different extents, depending on the location of the measured points, the origin of which is not understood to date. Moreover, the crack formation observed in the membrane was located at the boundary between the area which shows low degradation and the highly degraded nonactive area.

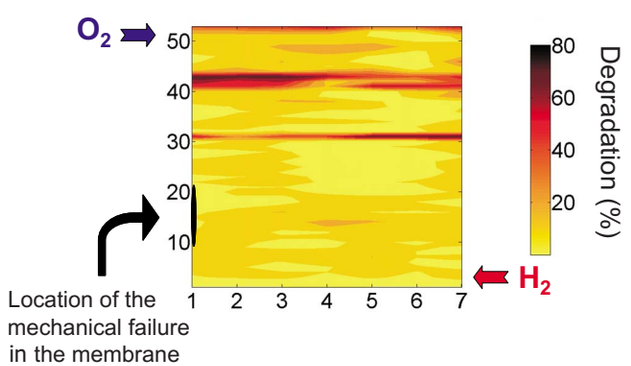

Figure 9. (Color online) Degradation map of the ETFE-based membrane within the active area.

Acknowledgments

The authors thank Manuel Arcaro, Friederike Geiger, and Christian Marmy for technical support. Funding by the Swiss Federal Office of Energy (SFOE) is gratefully acknowledged.

Paul Scherrer Institut assisted in meeting the publication costs of this article.

References

1. L. Gubler, S. A. Gürsel, and G. G. Scherer, *Fuel Cells*, **5**, 317 (2005).
2. L. Gubler, H. Kuhn, T. J. Schmidt, G. G. Scherer, H. P. Brack, and K. Simbeck, *Fuel Cells*, **4**, 196 (2004).
3. T. J. Schmidt, K. Simbeck, and G. G. Scherer, *J. Electrochem. Soc.*, **152**, A93 (2005).
4. H. P. Brack, F. N. Büchi, J. Huslage, M. Rota, and G. G. Scherer, in *ACS Symposium Series*, ACS, pp. 174–188 (2000).
5. L. Gubler, N. Prost, S. A. Gürsel, and G. G. Scherer, *Solid State Ionics*, **176**, 2849 (2005).
6. S. A. Gürsel, H. Ben youcef, A. Wokaun, and G. G. Scherer, *Nucl. Instrum. Methods Phys. Res. B*, **265**, 198 (2007).
7. H. Ben youcef, S. A. Gürsel, A. Wokaun, and G. G. Scherer, *J. Membr. Sci.*, **311**, 208 (2008).
8. A. B. LaConti, M. Hamdan, and R. C. McDonald, in *Handbook of Fuel Cells-Fundamentals, Technology and Applications*, W. Vielstich, H. A. Gasteiger, and A. Lamm, Editors, Vol. 3, John Wiley & Sons, Chichester (2003).
9. H. Ben youcef, S. A. Gürsel, A. Buisson, A. Wokaun, and G. G. Scherer, To be submitted.
10. S. A. Gürsel, Z. Yang, B. Choudhury, M. G. Roelofs, and G. G. Scherer, *J. Electrochem. Soc.*, **153**, A1964 (2006).
11. L. Gubler, M. Slaski, A. Wokaun, and G. G. Scherer, *Electrochem. Commun.*, **8**, 1215 (2006).
12. L. Gubler, H. Ben youcef, S. A. Gürsel, A. Wokaun, and G. G. Scherer, *J. Electrochem. Soc.*, **155**, B921 (2008).
13. T. Yamaki, J. Tsukada, M. Asano, R. Katakai, and M. Yoshida, *J. Fuel Cell Sci. Technol.*, **4**, 56 (2007).
14. L. Gubler, R. Müller, and G. G. Scherer, *PSI Electrochemistry Laboratory–Annual Report 2006*, ISSN 1661-5379, p. 19 (2006) (also available at http://ecl.web.psi.ch/SciRep.html).
15. R. Okasha, G. Hild, and P. Rempp, *Eur. Polym. J.*, **15**, 975 (1979).
16. B. Walczynski, B. N. Kolarz, and H. Galina, *Polym. Commun.*, **26**, 276 (1985).
17. S. Holmberg, J. Näsman, and F. Sundholm, *Polym. Adv. Technol.*, **9**, 121 (1998).
18. B. Mattsson, H. Ericson, L. M. Torell, and F. Sundholm, *Electrochim. Acta*, **45**, 1405 (2000).
19. G. Hübner and E. Roduner, *J. Mater. Chem.*, **9**, 409 (1999).
20. F. N. Büchi, B. Gupta, O. Haas, and G. G. Scherer, *Electrochim. Acta*, **40**, 345 (1995).
21. F. N. Büchi and G. G. Scherer, *J. Electrochem. Soc.*, **148**, A183 (2001).

22. J. Chen, M. Asano, T. Yamaki, and M. Yoshida, *J. Appl. Polym. Sci.*, **100**, 4565 (2006).
23. H.-P. Brack, D. Fischer, G. Peter, M. Slaski, and G. G. Scherer, *J. Polym. Sci., Part A: Polym. Chem.*, **42**, 59 (2003).
24. M. Slaski, L. Gubler, G. G. Scherer, and A. Wokaun, in *PSI Scientific Report 2004*, Vol. V, ISSN 1423-7342, Villigen, Switzerland, p. 114 (2004).
25. L. Gubler and G. G. Scherer, in *Handbook of Fuel Cells–Fundamentals, Technology and Applications*, W. Vielstich, H. A. Gasteiger and H. Yokokawa, Editors, Vol. 5, John Wiley & Sons, Chichester (2009).
26. S. A. Freunberger, M. Reum, J. Evertz, A. Wokaun, and F. N. Büchi, *J. Electrochem. Soc.*, **153**, A2158 (2006).
27. F. N. Büchi and M. Reum, *Meas. Sci. Technol.*, **19**, 085702 (2008).
28. B. Sompalli, B. A. Litteer, W. Gu, and H. A. Gasteiger, *J. Electrochem. Soc.*, **154**, B1349 (2007).